ISSN 1674-1056
http://cpb.iphy.ac.cn
http://iopscience.iop.org/cpb
中国物理 B
Chinese Physics
中国物理 Chinese Physics B

Multicaloric and coupled-caloric effects

Jia-Zheng Hao(郝嘉政), Feng-Xia Hu(胡凤霞), Zi-Bing Yu(尉紫冰), Fei-Ran Shen(沈斐然), Hou-Bo Zhou(周厚博), Yi-Hong Gao(高怡红), Kai-Ming Qiao(乔凯明), Jia Li(李佳), Cheng Zhang(张丞), Wen-Hui Liang(梁文会), Jing Wang(王晶), Jun He(何峻), Ji-Rong Sun(孙继荣), Bao-Gen Shen(沈保根)

Citation: Chin. Phys. B . 2020, 29(4): 047504 . **doi:** 10.1088/1674-1056/ab7da7
Journal homepage: http://cpb.iphy.ac.cn; http://iopscience.iop.org/cpb

What follows is a list of articles you may be interested in

Giant low-field magnetocaloric effect in $EuTi_{1-x}Nb_xO_3$ (x=0.05, 0.1, 0.15, and 0.2) compounds

Wen-Hao Jiang(姜文昊), Zhao-Jun Mo(莫兆军), Jia-Wei Luo(罗佳薇), Zhe-Xuan Zheng(郑哲轩), Qiu-Jie Lu(卢秋杰), Guo-Dong Liu(刘国栋), Jun Shen(沈俊), Lan Li(李岚)

Chin. Phys. B . 2020, 29(3): 037502 . **doi:** 10.1088/1674-1056/ab69e7

Magnetoresistance hysteresis in topological Kondo insulator SmB_6 nanowire

Ling-Jian Kong(孔令剑), Yong Zhou(周勇), Hua-Ding Song(宋化鼎), Da-Peng Yu(俞大鹏), Zhi-Min Liao(廖志敏)

Chin. Phys. B . 2019, 28(10): 107501 . **doi:** 10.1088/1674-1056/ab3a89

Critical behavior and magnetocaloric effect in magnetic Weyl semimetal candidate $Co_{2-x}ZrSn$

Tianlin Yu(于天麟), Xiaoyun Yu(余骁昀), En Yang(杨恩), Chang Sun(孙畅), Xiao Zhang(张晓), Ming Lei(雷鸣)

Chin. Phys. B . 2019, 28(6): 067501 . **doi:** 10.1088/1674-1056/28/6/067501

Magnetic properties and magnetocaloric effects in $(Ho_{1-x}Y_x)_5Pd_2$ compounds

X F Wu(武小飞), C P Guo(郭翠萍), G Cheng(成钢), C R Li(李长荣), J Wang(王江), Y S Du(杜玉松), G H Rao(饶光辉), Z M Du(杜振民)

Chin. Phys. B . 2019, 28(5): 057502 . **doi:** 10.1088/1674-1056/28/5/057502

Ferromagnetism and magnetostructural coupling in V-doped MnNiGe alloys

Hui Yang(杨慧), Jun Liu(刘俊), Chao Li(李超), Guang-Long Wang(王广龙), Yuan-Yuan Gong(龚元元), Feng Xu(徐锋)

Chin. Phys. B . 2018, 27(10): 107502 . **doi:** 10.1088/1674-1056/27/10/107502

TOPICAL REVIEW — Magnetism, magnetic materials, and interdisciplinary research

Multicaloric and coupled-caloric effects*

Jia-Zheng Hao(郝嘉政)[1,2], Feng-Xia Hu(胡凤霞)[2,3,4,†], Zi-Bing Yu(尉紫冰)[2,3], Fei-Ran Shen(沈斐然)[2,3], Hou-Bo Zhou(周厚博)[2,3], Yi-Hong Gao(高怡红)[2,3], Kai-Ming Qiao(乔凯明)[2,3], Jia Li(李佳)[2,3], Cheng Zhang(张丞)[2,3], Wen-Hui Liang(梁文会)[2,3], Jing Wang(王晶)[2,3,5], Jun He(何峻)[1,‡], Ji-Rong Sun(孙继荣)[2,3,4], and Bao-Gen Shen(沈保根)[2,3,4]

[1] *Division of Functional Material Research, Central Iron and Steel Research Institute, Beijing* 100081, *China*
[2] *Beijing National Laboratory for Condensed Matter Physics & State Key Laboratory of Magnetism, Institute of Physics, Chinese Academy of Sciences, Beijing* 100190, *China*
[3] *School of Physical Sciences, University of Chinese Academy of Sciences, Beijing* 100049, *China*
[4] *Songshan Lake Materials Laboratory, Dongguan* 523808, *China*
[5] *Fujian Innovation Academy, Chinese Academy of Sciences, Fuzhou* 350108, *China*

(Received 1 February 2020; revised manuscript received 20 February 2020; accepted manuscript online 9 March 2020)

The multicaloric effect refers to the thermal response of a solid material driven by simultaneous or sequential application of more than one type of external field. For practical applications, the multicaloric effect is a potentially interesting strategy to improve the efficiency of refrigeration devices. Here, the state of the art in multi-field driven multicaloric effect is reviewed. The phenomenology and fundamental thermodynamics of the multicaloric effect are well established. A number of theoretical and experimental research approaches are covered. At present, the theoretical understanding of the multicaloric effect is thorough. However, due to the limitation of the current experimental technology, the experimental approach is still in progress. All these researches indicated that the thermal response and effective reversibility of multiferroic materials can be improved through multicaloric cycles to overcome the inherent limitations of the physical mechanisms behind single-field-induced caloric effects. Finally, the viewpoint of further developments is presented.

Keywords: multicaloric effect, coupled-caloric effect, solid-state refrigeration, magnetocaloric effect

PACS: 05.70.Fh, 65.40.gd, 75.30.Sg, 75.85.+t **DOI:** 10.1088/1674-1056/ab7da7

1. Introduction

Solid-state refrigeration technology based on the caloric effects has superior refrigeration efficiency while reducing ozone consumption or greenhouse gas emissions. Therefore, it provides an energy-saving and environmentally-friendly refrigeration solution to replace the current mainstream vapor compression refrigeration technology.[1–6] The caloric effect of a solid refers to the reversible thermal change (isothermal change of entropy or adiabatic change of temperature) of the solid under the application of an external stimulus field, which generally occurs in the vicinity of phase transitions. The known caloric effects mainly include magnetocaloric effects,[1–6] electrocaloric effects,[7] and mechanical caloric effects (barocaloric[8] and elastocaloric effects[9]), which correspond to magnetic, electric, and mechanical fields (hydrostatic pressure and uniaxial stress), respectively. Multiferroic materials show two or more ferroic orders, and when the couplings of these ferroic orders are strong enough, each ferroic order can respond to more than one type of applied field. In addition, multiple ferroic phase transitions may occur at a nearby temperature. Therefore, it is expected that most giant magnetocaloric and electrocaloric materials will also exhibit mechanocaloric effects, since the magnetic and polar orders in such materials are strongly coupled to the lattice order.[10] The magnetocaloric, electrocaloric, or mechanocaloric effect will directly affect each other due to the cross-response to the magnetic/electric or mechanical field. Some studies have shown that the multicaloric effect driven by multiple fields may yield larger caloric response compared to the caloric effect induced by a single stimulus.[11–17]

So far, the study of single-field induced solid-state caloric effects has attracted widespread attention. In particular, giant magnetocaloric effects are generally observed when the ferroic phase transition is first order in nature.[18–27] Many studies have focused on achieving stronger magnetic first-order transitions, that is, achieving the greatest latent heat and the strongest magnetic–structural coupling. This method is beneficial to achieve higher caloric performance, especially large entropy changes. However, it is accompanied by many disad-

*Project supported by the National Key Research and Development Program of China (Grant Nos. 2017YFB0702702, 2019YFA0704904, 2018YFA0305704, 2017YFA0206300, 2017YFA0303601, and 2016YFB0700903), the National Natural Science Foundation of China (Grant Nos. U1832219, 51531008, 51771223, 51590880, 51971240, 11674378, 11934016, and 11921004), and the Key Program and Strategic Priority Research Program (B) of the Chinese Academy of Sciences.

†Corresponding author. E-mail: fxhu@iphy.ac.cn
‡Corresponding author. E-mail: hejun@cisri.com.cn

© 2020 Chinese Physical Society and IOP Publishing Ltd

vantages, such as large hysteresis loss, irreversibility of caloric effects, or poor mechanical stability. These definite drawbacks have limited the practical application and further development of the first-order transition materials in solid-state refrigeration. Considerable efforts have recently been made to overcome these problems.[28–34] Recent studies indicated that the hysteresis loss of materials can be reduced or even eliminated by utilizing the response of multiferroic materials to more than one type of driving field.[29,30,32] These studies have led to an enthusiastic search for multicaloric cycle and have encouraged fast-growing research activities in the field. The theoretical framework for multicaloric effect has been studied in sufficient detail.[16,17,35–37] However, due to the limitation of the current experimental technology, quite few experimental efforts have been devoted to the study of these combined magneto–mechanic or electro–mechanic caloric effects with the coupled term considered.[15,17,38] At present, most of the reported results involve studies on the effects of mechanical stress on the magnetocaloric and electrocaloric effects, while a small amount focus on the regulation of electro-induced strain on the magnetocaloric effect in magnetostructural coupled materials. Furthermore, cryogenic rare earth-based alloys and intermetallic compounds are mainly second order materials showing considerable magnetocaloric effect (MCE),[4,5,39–44] such as R–T (R = rare earth element; T = Fe, Co, Ni, Zn, and Ga) compounds,[5,45–54] ternary RTX (T = Fe, Co, and Pt; X = Al, Mg, and C) compounds,[55–60] ternary R_2T_2Al (T = Co, Ni, and Cu) and R_2Ni$_2$In compounds,[41,61,62] ternary R_4TX (T = Co, Pd, and Pt; X = Mg and Cd) compounds,[63,64] and quaternary RNi$_2$B$_2$C and RNiBC compounds.[65] However, some of these rare earth-based MCE materials still undergo unneglectable spin–lattice coupling, though the thermal and magnetic hysteresis may be approaching zero. For example, the spin orientation transition is occasionally accompanied by an abnormal lattice change, and a stress can also shift the transition. Because the experimental studies on the multicaloric and coupled-caloric effects are still limited, there are no relative reports involving the rare earth-based MCE materials up to now. Therefore, in this article the review mainly focuses on the multicaloric effect and coupled-caloric effect in the materials with significant characteristics of first-order transition.

In this article, we present a brief review of the state of the art in research on multicaloric materials and multicaloric effects. The phenomenology and fundamental thermodynamics of the multicaloric effect are reviewed, including some common theoretical and experimental approaches to study the multicaloric effect and coupled-caloric effect. Finally, the viewpoint of further developments is presented.

2. Thermodynamics of multicaloric effect

The ferroic material can be characterized by ferroic property X_i. with corresponding thermodynamically conjugated field x_i. These pairs of variables can be magnetization M and magnetic field H, polarization P and electric field E, or strain ε and stress σ. The caloric effects caused by the finite changes in the field x_i (keeping the remaining fields constant) are usually quantified by the entropy changes that occur when the field is applied or removed isothermally, and the temperature changes that occur when the field undergoes an adiabatic change. The isothermal change of the field-induced entropy can be obtained by integrating the appropriate Maxwell equation[15,17,36,37]

$$\Delta S(T,0\rightarrow x_i)=S(T,x_i)-S(T,0)=\int_0^{x_i}\left(\frac{\partial X_i}{\partial T}\right)_{x_i}\mathrm{d}x_i. \quad (1)$$

When the field is varied adiabatically, the entropy is constant. The adiabatic temperature change can be obtained by the following equation:

$$\Delta T(0\rightarrow x_i)=T(S,x_i)-T(S,0)=-\int_0^{y_i}\frac{T}{C}\left(\frac{\partial X_i}{\partial T}\right)_{x_i}\mathrm{d}x_i. \quad (2)$$

Multiferroic materials display two or more of the non-independence ferroic properties, and they may be strongly coupled. The multicaloric effects occur when more than one field is either simultaneously or sequentially applied. For the sake of clarity and practical applications, the system is considered with two ferroic properties X_1 and X_2 with thermodynamically conjugated fields x_1 and x_2, respectively. In general, for adiabatic temperature changes, it is easy to obtain similar expressions to that obtained for isothermal entropy changes. Similar to the caloric effect induced by a single field in an equilibrium thermodynamic system, the multicaloric effect can also be quantified by the isothermal entropy change. Furthermore, the entropy is a state function, so the magnitude of the isothermal entropy change is independent of the thermodynamic path of the applied multiple external fields, and it does not depend on whether the driving fields are applied simultaneously or sequentially. Assuming the system responds isotropically to the applied field, the change in entropy caused by the isothermal change in the two fields can be expressed as[15,17,36,37]

$$\begin{aligned}&\Delta S[T,(0,0)\rightarrow(x_1,x_2)]\\&=\Delta S[T,(0,0)\rightarrow(x_1,0)]+\Delta S[T,(x_1,0)\rightarrow(x_1,x_2)].\end{aligned} \quad (3)$$

The first term on the right is only a single field-induced entropy change that quantifies the caloric effect related to the ferroic property X_1

$$\Delta S[T,(0,0)\rightarrow(x_1,0)]=\int_0^{x_1}\left(\frac{\partial X_1}{\partial T}\right)_{x_1,x_2=0}\mathrm{d}x_1, \quad (4)$$

while the second term on the right is the caloric effect due to the application of field x_2 at constant x_1, and it can be written as the sum of terms of the single caloric effect associated

with the induced change of the property X_2 and a caloric cross-response contribution

$$\begin{aligned}&\Delta S[T,(x_1,0)\to(x_1,x_2)]\\&=\Delta S[T,(0,0)\to(0,x_2)]\\&\quad+\int_0^{x_1}\frac{\partial}{\partial x_1'}\left[\Delta S\left[T,(x_1',0)\to(x_1',x_2)\right]\right]\mathrm{d}x_1'\\&=\int_0^{x_2}\left(\frac{\partial X_2}{\partial T}\right)_{x_1=0,x_2}\mathrm{d}x_2+\int_0^{x_1}\int_0^{x_2}\frac{\partial\chi_{12}}{\partial T}\mathrm{d}x_2\mathrm{d}x_1,\end{aligned}\tag{5}$$

where $\chi_{12}=(\partial X_1/\partial x_2)_{T,x_1}=(\partial X_2/\partial x_1)_{T,x_2}$ is the cross-susceptibility that quantifies the response of X_1 (X_2) to the nonconjugated field x_2 (x_1). It indicates the strength of the interaction between ferroic properties X_1 and X_2. Therefore, due to the interaction between ferroic properties X_1 and X_2, the multicaloric effect is not a simple sum of the caloric effects associated with each one alone. The isothermal entropy change of the multicaloric effect can be written as

$$\begin{aligned}&\Delta S[T,(0,0)\to(x_1,x_2)]\\&=\int_0^{x_1}\left(\frac{\partial X_1}{\partial T}\right)_{x_1,x_2=0}\mathrm{d}x_1+\int_0^{x_2}\left(\frac{\partial X_2}{\partial T}\right)_{x_1=0,x_2}\mathrm{d}x_2\\&\quad+\int_0^{x_1}\int_0^{x_2}\frac{\partial\chi_{12}}{\partial T}\mathrm{d}x_2\mathrm{d}x_1,\end{aligned}\tag{6}$$

where the last coupled term produces the coupled-caloric effect.

Another useful method for proving the interdependence of thermal response on different external fields is to analyze the caloric effects caused by changes in the ferroic property X_i on the application or removal of the non-conjugated field x_j, and maintain the remaining fields constant. The ferroic property can be expressed as $X_i=X_i(T,x_1,x_2)$, where $i=1,2$. One may then express the entropy change by the appropriate Maxwell relations as follows:[15,17,36,37]

$$\begin{aligned}&\Delta S[T,x_1=0,X_1(0)\to X_1(x_2)]\\&=-\int_{X_1(0)}^{X_1(x_2)}\left(\frac{\partial x_1}{\partial T}\right)_{X_1,X_2}\mathrm{d}X_1,\end{aligned}\tag{7}$$

where $X_1(0)$ and $X_1(x_2)$ are the values of the X_1 variable at $x_2=0$ and at a given value of the field x_2, respectively. Taking into account that

$$\left(\frac{\partial x_1}{\partial T}\right)_{X_1}=-\left(\frac{\partial x_1}{\partial X_1}\right)_T\left(\frac{\partial X_1}{\partial T}\right)_{x_1},\tag{8}$$

and $\mathrm{d}X_1=\left(\frac{\partial X_1}{\partial x_2}\right)\mathrm{d}x_2$, from Eqs. (6)–(8), the entropy change $\Delta S[T,x_1=0,X_1(0)\to X_1(x_2)]$ can be expressed as

$$\begin{aligned}&\Delta S[T,x_1=0,X_1(0)\to X_1(x_2)]\\&=\int_0^{x_2}\frac{\left(\frac{\partial X_1}{\partial x_2}\right)}{\left(\frac{\partial x_1}{\partial X_1}\right)_T}\left(\frac{\partial X_1}{\partial T}\right)_{x_1=0,x_2}\mathrm{d}x_2.\end{aligned}\tag{9}$$

3. Theoretical approaches

3.1. First-principles calculations

First-principles calculation plays a very fruitful role in the theoretical understanding of the multicaloric effect. Lisenkov *et al.* used first-principles simulations to study the multicaloric effect in a typical ferroelastic/ferroelectric $PbTiO_3$, providing insights into the multicaloric effect of the material.[16] To explore the multicaloric nature of $PbTiO_3$, they used the direct approach[66,67] to calculate the caloric change directly. The total energy of $PbTiO_3$ is given by the effective Hamiltonian by the first-principles calculation. This Hamiltonian correctly predicts various structural and thermodynamic properties of $PbTiO_3$, including polarization, Curie temperature, and some others. In addition, the total energy given by the Hamiltonian was used in the framework of an isenthalpic Monte Carlo simulation, which simulates the electrocaloric effect induced by a single electric field, the barocaloric effect induced by a single stress field, and the multicaloric effect induced by the electric field and pressure simultaneously. Their work found that the multicaloric effect far exceeds either piezocaloric or electrocaloric effect in the same material. In addition, when multiple external fields are applied, the strong coupling between the two ferroic order parameters plays a key role in the significant enhancement of the caloric effect. This study clearly shows that first-principles calculations are of great significance for understanding the multicaloric effect from a theoretical perspective.

3.2. Landau theory

The Landau model can also be used to describe the multiple thermal properties near phase transitions in the system. This model combines the coupling between the ordered parameters related to two ferroic properties. Planes *et al.* discussed the multicaloric effect under the combined action of a magnetic field and an electric field based on a system with a magnetoelectric coupling.[37,68] The related order parameters are the magnetization M and the polarization P. Therefore, the proposed Landau free energy contains pure terms related to the polar and magnetic contributions and terms that explain their interaction. That is, the free energy can be expressed as

$$F=F_P(T,P)+F_M(T,M)+F_{P-M}(P,M).\tag{10}$$

In the Laudau phase transition theory, the following free energy contributions can be obtained:

$$F_P(T,P)=F_P(T)+\frac{1}{2}aP^2+\frac{1}{4}bP^4+\frac{1}{6}cP^6+\cdots,\tag{11}$$

$$F_M(T,M)=F_M(T)+\frac{1}{2}\alpha M^2+\frac{1}{4}\beta M^4+\frac{1}{6}\gamma M^6+\cdots,\tag{12}$$

$$F_{P-M}(P,M)=\frac{1}{2}\kappa P^2M^2,\tag{13}$$

where κ represents the magnetoelectric coefficient. Furthermore, according to the Curie–Weiss law,

$$a = \chi_P^{-1} = \eta_P(T - T_c^P), \tag{14}$$

$$\alpha = \chi_M^{-1} = \eta_M(T - T_c^M), \tag{15}$$

where T_c^P and T_c^M are the paraelectric transition temperature and paramagnetic Curie temperature, respectively.

They assumed $b > 0$, $\beta > 0$, and $\gamma > 0$ to ensure that the pure ferroelectric and ferromagnetic free energy functions are positive definitely for large values of P and M. Electric field E and magnetic field H can be introduced by introducing Gibbs-like polar and magnetic free energies

$$G_P = F_P - EP, \tag{16}$$

$$G_M = F_M - HM. \tag{17}$$

The minimum of the Gibbs free energy $G = G_P + G_M + F_{P-M}$ relative to P gives the relationship between P and M,

$$bP^3 + aP + \kappa PM^2 = E. \tag{18}$$

When the applied electric field is zero, the following relationship exists in the ferroelectric phase:

$$P^2 = -(a + \kappa M^2)/b. \tag{19}$$

Therefore, the effective magnetic Gibbs free energy can be expressed as

$$G_{\text{eff}} = G_0(T) + \frac{1}{2}A(T,\kappa)M^2 + \frac{1}{4}B(\kappa)M^4 + \frac{1}{6}\gamma M^6 - HM,$$

with

$$G_0(T) = -\frac{a(T)^2}{4b}, \quad A(T,\kappa) = \alpha(T) - \kappa\frac{a(T)}{b},$$
$$B(\kappa) = \beta - \frac{\kappa^2}{b}. \tag{20}$$

From the Landau phase transition theory, the sign of the fourth-order coefficient $B(\kappa)$ predicts that the magnetoelectric phase transition might be continuous or discontinuous. According to the above model, Plane *et al.* established a phase diagram of the magnetoelectric coupling coefficient and temperature, and pointed out that the slope of the coexistence line in the E–H diagram at a given temperature can be given by the generalized Clausius–Clapeyron equation in a first-order phase transition material

$$\frac{\mathrm{d}E}{\mathrm{d}H} = -\frac{\Delta M}{\Delta P}. \tag{21}$$

The pure electrocaloric effect can be obtained by the following equation:

$$\begin{aligned} &S(T, 0 \to E) \\ &= -\frac{\partial G_P}{\partial T} = S_0(T) - \frac{1}{2}\eta_P P^2(T,E) \\ &= -\frac{1}{2}\eta_P\left[P^2(T,E) - P^2(T,0)\right] = \int_0^E \left(\frac{\partial P}{\partial T}\right)_E \mathrm{d}E, \end{aligned} \tag{22}$$

where $S_0(T) = a(T)/(2b)$ and $P^2(T,E)$ is a solution of $\partial G_P/\partial P = 0$. In addition, at constant temperature, $(\partial P/\partial T)_E \mathrm{d}E = -\eta_P P \mathrm{d}P$.

Furthermore, the isothermal entropy change induced by the magnetic field H can be expressed as the sum of the polar and magnetic contributions

$$\begin{aligned} &\Delta S(T, E = 0, 0 \to H) = \Delta S_P[T, E = 0, P(0) \to P(H)] \\ &+ \Delta S_M[T, E = 0, M(0) \to M(H)], \end{aligned} \tag{23}$$

where the cross-caloric term associated with the polar induced by the magnetic field is given by

$$\begin{aligned} &\Delta S_P[T, E = 0, P(0) \to P(H)] = S_P(T,H) - S_0(T,0) \\ &= \frac{1}{2}\eta_P\frac{\kappa}{b}\left[M^2(T,H) - M^2(T,0)\right], \end{aligned} \tag{24}$$

and the pure magnetic contribution is given by

$$\begin{aligned} &\Delta S_M[T, E = 0, M(0) \to M(H)] = S_M(T,H) - S_M(T,0) \\ &= -\frac{1}{2}\eta_M\left[M^2(T,H) - M^2(T,0)\right]. \end{aligned} \tag{25}$$

Therefore, the isothermal entropy change of the multicaloric effect induced by the simultaneous application of magnetic and electric fields can be obtained as

$$\begin{aligned} &\Delta S(T, 0 \to E, 0 \to H) \\ &= \Delta S(T, E = 0, 0 \to H) + \Delta S(T, 0 \to E, H), \end{aligned} \tag{26}$$

where

$$\begin{aligned} &\Delta S(T, 0 \to E, H) \\ &= -\frac{\partial}{\partial T}\left\{G_{\text{eff}}[T, M(H,E)] - G_{\text{eff}}[T, M(H,0)]\right\}, \end{aligned}$$

in this case, the relationship between P and M can be given by Eq. (19), and $M(H,E)$ is the solution of $\partial G_{\text{eff}}/\partial M = \partial F_{\text{eff}}/\partial M - H = 0$.

Plane *et al.* used these expressions to investigate the multicaloric effect within Landau theory.[36,37] The authors found that the application of both magnetic and electric fields can improve the whole effect when both the magnetic and polar contributions are conventional. In other words, when the signs of the entropy change of caloric effect induced by the magnetic field and the electric field are opposite, the magnitude of the multicaloric effect will be lower than that of the caloric effect induced by a certain single field.[36] They also analyzed the multicaloric effect in the magnetostructural metamagnetic shape-memory materials with a Landau model. Their phenomenological Landau results combined with first-principle calculations provide a route for designing materials with improved multicaloric effects.[37] Furthermore, several authors have studied the ferroelastic/ferroelectric single

crystals within this framework.[35,69] Liu *et al.* reported the multicaloric effect in $BaTiO_3$ single crystals driven simultaneously by mechanical and electric fields, which was described via the Landau free-energy model. They found that the multicaloric behavior is mainly dominated by the mechanical field rather than the electric field, since the paraelectric-to-ferroelectric transition is more sensitive to the mechanical field than to the electric field.[35] Meng *et al.* used a phenomenological calculation based on the Landau phase transition theory to evaluate the magnitude of the coupled-caloric effect in a ferromagnetic–ferroelectric system. Their results indicated that the magneto-electric coupling greatly strengthens the magnetization, ferroelectric polarization, and isothermal entropy change in the coupled ferromagnetic-ferroelectric multiferroic system. The caloric effect in the coupled system is greatly enhanced by increasing the magneto-electric coupling strength.[69]

3.3. Mean field model

To describe the muticaloric effect of specific materials in more detail, a reliable approach is to consider the mean field model which captures the internal mechanism expected to be more important. Stern-Taulats *et al.* used the mean field model for the free energy of the FeRh bulk to describe the antiferromagnetic (AFM) to ferromagnetic (FM) phase transition.[17] The model includes a magnetovolumic coupling term to account for the changes in unit cell volume during transition, and the coupling term includes the effect of external fields such as pressure P and magnetic field H. The total free energy of the system is $f = f_{\rm mag} + f_{\rm coupling}$, and the variational Gibbs energy function per magnetic atom is

$$\begin{aligned} g^* = \frac{g}{zJ^{(1)}_{\rm FeRh}} &= -\frac{1}{2}m_{\rm Fe}m_{\rm Rh} - \frac{J^*}{4}\left(m^2_{\rm Fe} - \eta^2_{\rm Fe}\right) \\ &+ \frac{T^*}{8}[(1+m_{\rm Fe}+\eta_{\rm Fe})\ln(1+m_{\rm Fe}+\eta_{\rm Fe}) \\ &+ (1-m_{\rm Fe}-\eta_{\rm Fe})\ln(1-m_{\rm Fe}-\eta_{\rm Fe}) \\ &+ (1+m_{\rm Fe}-\eta_{\rm Fe})\ln(1+m_{\rm Fe}-\eta_{\rm Fe}) \\ &+ (1-m_{\rm Fe}+\eta_{\rm Fe})\ln(1-m_{\rm Fe}+\eta_{\rm Fe}) \\ &+ 2(1+m_{\rm Rh})\ln(1+m_{\rm Rh}) \\ &+ 2(1-m_{\rm Rh})\ln(1-m_{\rm Rh}) - 8\ln 2] \\ &+ \frac{1}{2}\alpha^*_0\omega^2 - \alpha^*_1\omega(m_{\rm Fe}+m_{\rm Rh})^2 \\ &- \alpha^*_2\omega\eta^2_{\rm Fe} - H^*(m_{\rm Fe}+m_{\rm Rh}) + P\Omega^*_0\omega, \end{aligned} \tag{27}$$

where $m_{\rm Fe}$ and $m_{\rm Rh}$ are the order parameters that describe the ferromagnetism of the sublattices of Fe and Rh; $\eta_{\rm Fe}$ is the AFM order parameter of Fe; ω is the relative volume change; α_1 and α_2 are the magnetostriction coefficients, and α_0 is the inverse of the compressibility. J is an effective exchange interaction parameter and z refers to the coordination number of the first neighbors.

Therefore, the entropy S of the system can be directly computed from Eq. (27) by employing the thermodynamic definition of S,

$$\begin{aligned} &S(m_{\rm Fe}, m_{\rm Rh}, \eta_{\rm Fe}) \\ &= -[\partial g^*/\partial T^*]_{P,H} = S_{\rm Fe}(m_{\rm Fe}, \eta_{\rm Fe}) + S_{\rm Rh}(m_{\rm Rh}), \end{aligned} \tag{28}$$

where $m_{\rm Fe}(T,H,P)$, $m_{\rm Rh}(T,H,P)$, and $\eta_{\rm Fe}(T,H,P)$ are the equilibrium order parameters. The isothermal entropy change for the multicaloric effect induced by the application of pressure and magnetic field can be calculated from

$$\Delta S(T, 0\to H, 0\to P) = S(T,H,P) - S(T,H=0,P=0).$$

Stern-Taulats *et al.* also studied the multicaloric effect and the effects of hysteresis within this mean field approximation and the model also nicely reproduced the experimental data of the magnetostructural coupled system (bulk FeRh) over a broad range of pressure, magnetic field, and temperature.[17]

4. Experiment approaches

Previous theoretical studies have shown that the huge thermal response of a multiferroic material to an applied magnetic/electric field or stress originates from the strong coupling interaction between spin/polar and lattice. Due to the cross-response to mechanical, magnetic or electric fields, it is expected that the multicaloric effect driven by multiple fields can enhance the caloric effect and overcome some shortcomings such as the limitation of the cooling temperature window and irreversibilities due to hysteresis. However, most of previous experimental studies focused on the effect of hydrostatic pressure on the magnetocaloric effect and the electrocaloric effect. Hydrostatic pressure, as a clean means compared to chemical pressure, has been successfully used to tune the temperature position through impacting the magnetostructural/magnetoelastic transition for the giant MCE materials. However, the magnitude of MCE could be seldom enhanced by a physical pressure except for a few cases where the enhanced MCE mainly originates from the enhanced contribution of the lattice and the strengthening of the first-order transition by the pressure.[11–13] For example, the application of hydrostatic pressure on $Tb_5Si_2Ge_2$ compound[11] can significantly enhance the MCE by changing the phase transition from second-order to first-order in nature. Large enhancements of magnetocaloric and barocaloric effects by hydrostatic pressure were also observed in $La(Fe_{0.92}Co_{0.08})_{11.9}Si_{1.1}$ compound,[12] which mainly originate from the increased contribution of the lattice entropy change ($\Delta S_{\rm Latt}$). Neutron powder diffraction revealed that the hydrostatic pressure sharpens the magnetoelastic transition and enlarges the volume change, $\Delta V/V$, during the magnetoelastic transition through altering the specific atomic environments of $NaZn_{13}$-type structure.[12] For

the Ni_2In-type hexagonal $(MnNiSi)_{1-x}(MnFeGe)_x$ alloys, enhanced MCE by hydrostatic pressure was also observed, which was ascribed to the enlarged $\Delta V/V$ across the magnetostructural transition.[13] The estimated enhancement of $\Delta V/V$ is up to 7% by pressure according to the relation between the $\Delta S_{\rm Latt}$ and volume change $\Delta V/V$, i.e., $\delta[\Delta V/V(\%)]/\delta(\Delta S_{\rm Latt}) = 0.08\ {\rm J\cdot kg^{-1}\cdot K^{-1}}$.

Moreover, for the MCE materials with magnetostructural/magnetoelastic transition, the inherent hysteresis loss can be reduced through dual-field regulation or multicaloric cycle. For example, a reduction of magnetic hysteresis has been observed in Ni–Mn–In–Co bulk, where the sample is magnetized at ambient pressure while demagnetized under 1.3 kbar.[29] FeRh alloys have also been studied from this perspective. Liu *et al.* reduced the magnetic hysteresis loss by 96% in a dual-field magneric-electric refrigeration cycle for FeRh/$BaTiO_3$ heterostructures.[30] The multicaloric cycle gives rise to larger reversible caloric effect than any single field. The same situation was demonstrated in the multicaloric cycle of FeRh/PMN-PT heterostructure.[32] Qiao *et al.* reported a nonvolatile reduction of hysteresis loss in FeRh film, and quantitative analysis indicated that the effective refrigeration capacity ($RC_{\rm eff}$) can be increased to a new height by utilizing the external mechanical work as long as the nonvolatile strain can be large enough.

The findings discussed above provide important guidance for significantly enhancing the caloric effects and reducing the hysteresis loss through multi-field regulation. However, in these studies, the applied stress usually kept constant and the coupling term driven by the combined application of magnetic field and pressure was not taken into account. The main obstacle lies in the fact that it is difficult to realize a continuously changing stress field in reality. So far, only two experimental studies of multicaloric effect have considered the coupling terms, where the function of magnetization as pressure was obtained by a nonlinear numerical simulation based on the magnetization data collected under different pressures. One is the $Fe_{49}Rh_{51}$[17] and the other is the $Ni_{50}Mn_{35}In_{15}$ alloys.[15] However, it is worth noting that the pressure and magnetic fields have opposite effects on the magnetostructural transition for these two alloys. Currently, almost no study has been conducted on systems in which the magnetic field and hydrostatic pressure drive the phase transition in the same direction.

4.1. FeRh alloys

FeRh alloys have attracted considerable attention in recent years due to their large magnetocaloric,[70] elastocaloric,[71] and barocaloric[72] effects. FeRh is an ideal material for studying the fundamentals of multicaloric effect, which undergoes a magnetoelastic transition from a low temperature AFM to a high temperature FM phase. The crystal structure remains the CsCl-type cubic ($Pm3m$) but the lattice expands isotropically by $\Delta V/V \sim 1\%$ on heating during the transition for $Fe_{49}Rh_{51}$ alloys.[17,72] Therefore, the application of magnetic field and hydrostatic pressure has opposite effect on the magnetoelastic transition. The former drives the transition to low temperature while the latter drives the transition to high temperature (Fig. 1(a)). In other words, $Fe_{49}Rh_{51}$ exhibits inverse magnetocaloric effect and conventional barocaloric effect. A proper combination of pressure and magnetic field can not only achieve a significant broadening of the cooling temperature zone, but also reverse the sign of the entropy change from conventional to inverse. In 2015, Stern-Taulats *et al.*[17] performed magnetic measurements under different hydrostatic pressures, and then the relationship between the magnetization and the pressure (M–P curve) at a specific temperature was obtained by a nonlinear numerical simulation (Fig. 1(b)).

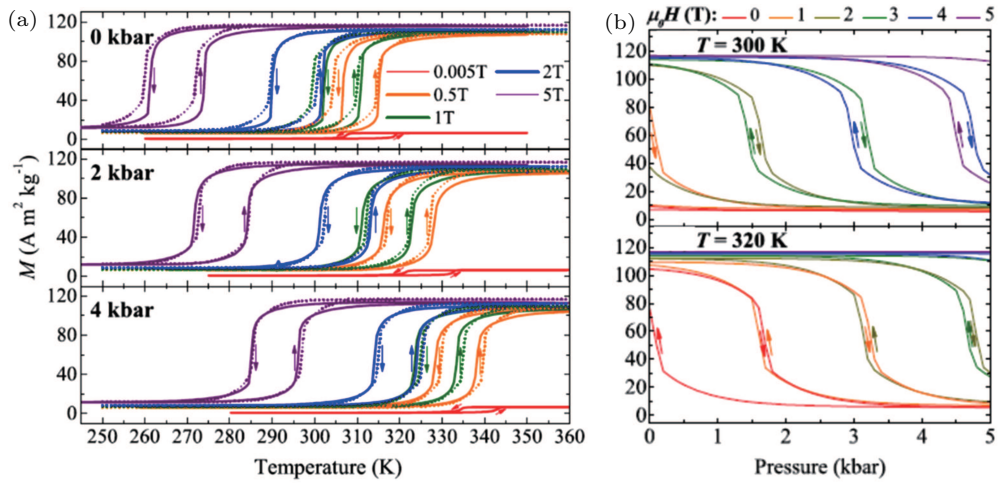


Fig. 1. (a) Thermomagnetic curves of $Fe_{49}Rh_{51}$ alloy under different magnetic fields and pressures. (b) Isothermal magnetization as a function of pressure for $Fe_{49}Rh_{51}$ at 300 K and 320 K. (Reprinted with permission from Ref. [17]. Copyright 2017, APS Publishing Limited).

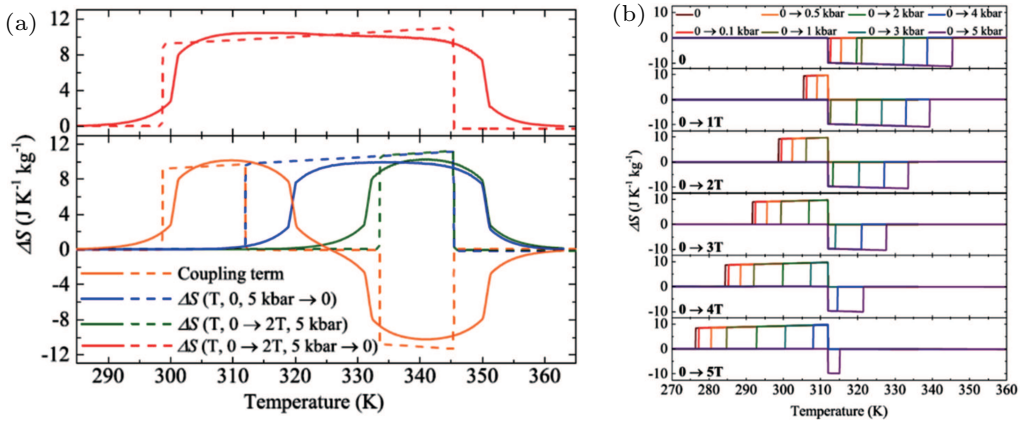


Fig. 2. (a) Temperature dependence of the multicaloric effect (red line), single barocaloric effect under zero magnetic field (blue line), single magnetocaloric effect at 5 kbar (green line), and the coupled-caloric effect (orange line) in $Fe_{49}Rh_{51}$ corresponding to the application of a 2 T magnetic field and the removal of 5 kbar pressure. (b) Temperature dependence of the multicaloric effect for combined application of magnetic field and hydrostatic pressure. (Reprinted with permission from Ref. [17]. Copyright 2017, APS Publishing Limited).

By using the thermodynamic relationship in Section 2, quantitative data of the entropy changes of the coupled-caloric and multicaloric effects were obtained based on the *M*–*P* curves. Figure 2 shows the temperature dependent entropy changes of multicaloric, single magnetocaloric, single barocaloric, and coupled-caloric effects under the combined application of hydrostatic pressure and magnetic field. It can be observed that, for the thermodynamic path where the magnetic field is applied and the pressure is removed, the single magnetocaloric (Fig. 2(a), green line) and the single barocaloric (Fig. 2(a), blue line) effects are both limited to a narrow temperature range. While the multicaloric effect (Fig. 2(a), red line) shows a significantly broadened cooling temperature region, which is contributed by the cross-response, i.e., the so called coupled-caloric effect (Fig. 2(a), orange line). However, for the thermodynamic path where the magnetic field and pressure are both applied at the same direction, the combination of the inverse magnetocaloric effect and the conventional barocaloric effect will produce a special multicaloric response in $Fe_{49}Rh_{51}$, as shown in Fig. 2(b). At lower magnetic fields, the conventional barocaloric effect plays a dominant role, and the application of pressure reduces the total entropy change. As the magnetic field increases, the effect of the inverse magnetocaloric effect gradually increases. When the magnetic field increases to a certain value, the sign of the multicaloric effect in $Fe_{49}Rh_{51}$ alloy changes from negative to positive, and the cooling temperature region shifts to lower temperature. It proves that, due to the different performance of the coupled-caloric effect, the sign of the multicaloric response can be finely adjusted by application of magnetic field and hydrostatic pressure. These performances of the thermodynamic path dependence of the multicaloric effect are closely related to the opposite effects of magnetic field and pressure on the phase transition. However, the physical mechanism of the coupled-caloric effect is not involved in this work, which requires further research.

4.2. Ni–Mn-based Heusler alloys

In order to further study the physical mechanism behind the coupled-caloric effect, Liang *et al.* investigated the coupled-caloric effect driven by combined hydrostatic pressure and magnetic field in $Ni_{50}Mn_{35}In_{15}$ alloy by using the measured magnetization data under different pressures.[15] It is worth noting that the driving direction of pressure for the martensitic magnetostructural transition of the off-stoichiometric Heusler alloy $Ni_2Mn_{1+x}In_{1-x}$ is also opposite to that of the magnetic field. The off-stoichiometric Heusler alloy $Ni_2Mn_{1+x}M_{1-x}$ (M = Ga, Sn and In, $0 < x < 1$) undergoes a martensitic transformation from a high temperature $L2_1$ cubic structure to a closely packed martensite phase with low crystal symmetry.[73] Many important functional properties related to the martensitic transition have been reported, such as metamagnetic shape memory effect,[74] magnetic superelasticity,[75] giant magnetocaloric effect, and magnetoresistance.[76] The application of hydrostatic pressure compresses the lattice and shortens the nearest neighboring atomic distance of Mn–Mn. As a response, the AFM exchange between the Mn atoms enhances, resulting in the shift of the martensitic transition temperature (T_M) to higher temperature.[77] Meanwhile, the alloys exhibit a big difference of magnetization between the FM austenitic and non-magnetic/PM martensitic phases near the transition temperature. The resultant large difference of Zeeman energy ensures that the martensitic transition can be driven to lower temperature by an external magnetic field.[78] Therefore, the off-stoichiometric $Ni_2Mn_{1+x}In_{1-x}$ is also an ideal platform for investigating the fundamentals of multicaloric effect driven by magnetic field and pressure. Studies indicated that,[15] in the temperature region of phase transition for $Ni_{50}Mn_{35}In_{15}$ alloy, the effect of pressure on magnetic properties can be expressed by the change of magnetic volume coupling coefficient χ_{12} caused by pressure. The macroscopic physical meaning of χ_{12} refers to the change of magnetism driven by the external pressure at a certain temperature

in the phase transition region. By measuring the thermomagnetic curves under different magnetic fields and pressures, the relationship between magnetization and pressure at a specific temperature (M–P curve) can be obtained by nonlinear fitting. Then, the magnetic volume coupling coefficient χ_{12} is derived from the M–P curves by the equation $\chi_{12} = (\partial M/\partial P)_{T,\mu_0 H}$. Figure 3 shows the colored contour map and two-dimensional (2D) plots of magnetic volume coupling coefficient χ_{12} as functions of pressure and temperature under 5 T magnetic field. With the increase of pressure, the peak position of χ_{12} gradually moves to higher temperature, and the peak always appears near $T_{\rm M}$ regardless of the pressure. It is worth noting that, according to Eq. (5), the coupled-caloric effect is the double integral of the magnetic volume coupling coefficient χ_{12} ($\Delta S_{\rm cp} = \int_0^P \int_0^H \partial\chi_{12}/\partial T \mathrm{d}H\mathrm{d}P$), so the evolution of χ_{12} with pressure and temperature directly reflects the characteristic behavior of the coupling caloric effect.

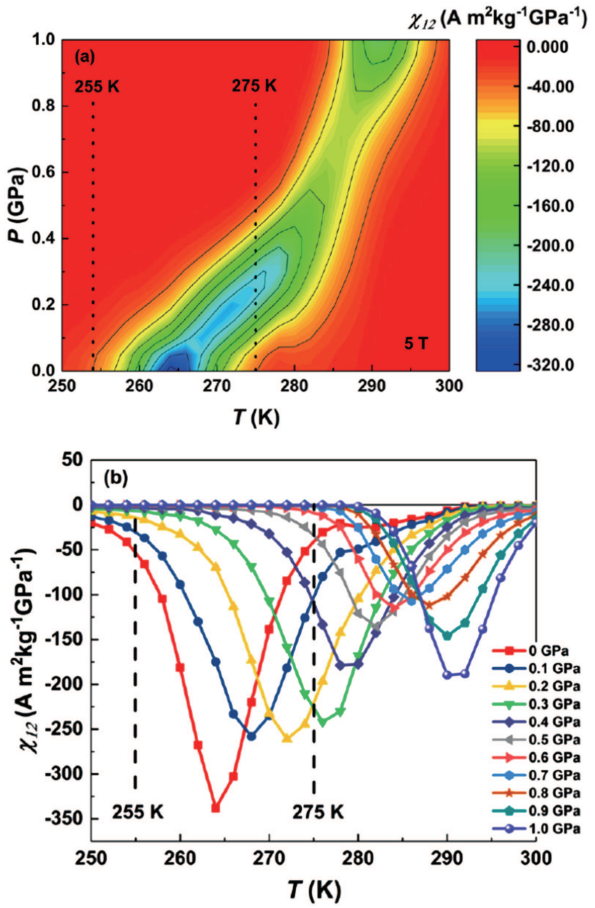


Fig. 3. (a) Colored contour map and (b) two-dimensional plots of magnetic volume coupling coefficient χ_{12} as functions of pressure and temperature. (Reprinted with permission from Ref. [15]; licensed under a Creative Commons Attribution (CC BY) license).

The coupled-caloric effects and magnetocaloric effects under certain pressure have been calculated based on the M–P and M–H curves using thermodynamic formulas in Section 2. The application of different pressures and the removal of magnetic field from 5 T to 0 were chosen as the thermodynamic path. For the entropy change of the coupled-caloric effect (Figs. 4(a) and 4(b)), a negative peak gradually increases in width and depth with increasing pressure near a low temperature of 264 K, while a positive peak forms in the high temperature region (Figs. 4(a) and 4(b)). In other words, the entropy change of the coupled-caloric effect shows a separation of positive and negative peaks. Comparison of the entropy change of the calculated and experimentally measured magnetocaloric effects indicates the caloric effect driven by magnetic field under a certain pressure is the magnetocaloric effect at ambient pressure adjusted by the coupled-caloric effect (Fig. 4(c)). The negative peak of the coupled-caloric effect in the low temperature range compensates the entropy change at ambient

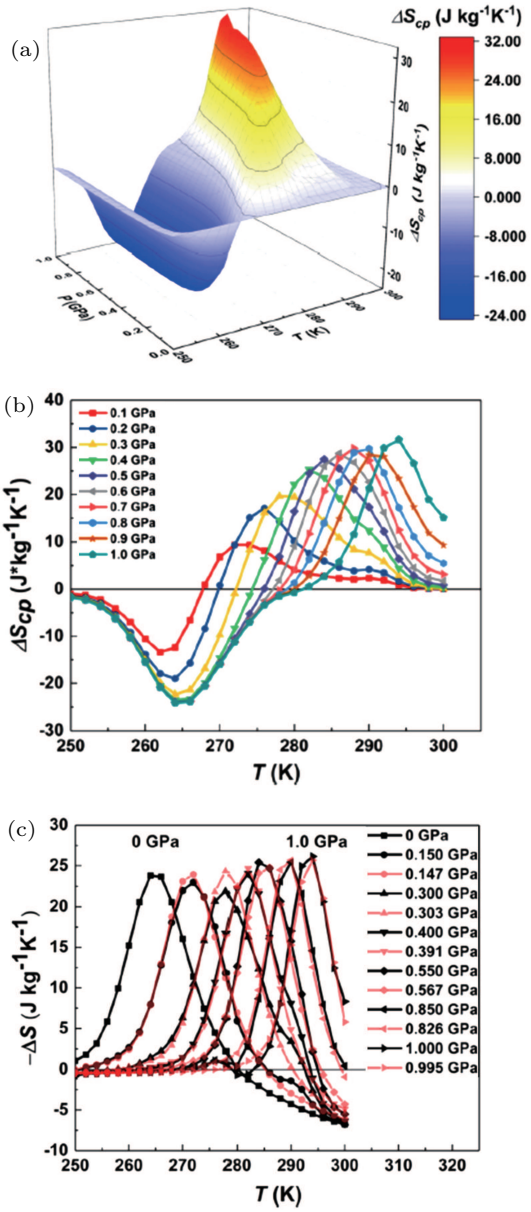


Fig. 4. (a) The 3D and (b) 2D plots of the coupled-caloric effect as a function of pressure and temperature for a magnetic field change of 5–0 T. (c) Comparison of the entropy change at ambient pressure adjusted by the coupled-caloric effect and the magnetocaloric results at a specific pressure calculated using Maxwell relation. (Reprinted with permission from Ref. [15]; licensed under a Creative Commons Attribution (CC BY) license).

pressure. While the positive peak of the coupled-caloric effect, which reflects the evolution of magnetic-structural coupling with pressure, contributes to the entropy change at high pressure. Although the pressure of 9.95 kbar reduces the change in magnetization (ΔM) across the T_M by 20%, the contribution of the coupled-caloric effect makes the magnetic entropy change enhanced by 8%. Via quantitatively analyzing the coupled-caloric effect, the essence of the regulated magnetocaloric effect by pressure is revealed in this work, which is of significance for designing new materials based on the magnetostructural coupling strength and its sensitivity to pressure.

5. Outlook

For the material with first-order transition, the multicaloric effect driven by multiple fields can overcome some inherent limitations of single caloric effect by improving its thermal response and reversibility. Quantitative analysis about the coupling term contributed to the multicaloric effect can promote the understanding of the refrigeration process controlled by multiple fields. Through pioneer efforts, the multicaloric effect can be understood theoretically in enough detail. However, due to the limitations of experimental technology, few experimental studies have focused on the coupled-caloric and multicaloric effects. The main obstacle lies in the fact that it is difficult to realize a continuously changing stress field in reality. So far, only two experimental studies of multicaloric effect have considered the coupling terms, where the function of magnetization as pressure was obtained by a nonlinear numerical simulation based on the magnetization data collected under different pressures. One is the $Fe_{49}Rh_{51}$ and the other is the $Ni_{50}Mn_{35}In_{15}$ alloys. Although the driving directions of magnetostructural/magnetoelastic transition by magnetic field and hydrostatic pressure are opposite for both alloys, a proper choice of the thermodynamic path can lead to an enhanced and broadened caloric response.

The entropy change of the coupled-caloric effect shows separated positive and negative peaks, and the sign of these two peaks depends on the thermodynamic path of the applied pressure and magnetic field. For the materials with opposite driving directions by magnetic field and hydrostatic pressure, the temperature span of the multicaloric effect can be significantly widened in a thermodynamic path where the magnetic field is applied and the pressure is removed; while, the sign of the multicaloric effect is turned over from negative to positive in the thermodynamic path where the magnetic field and pressure are both applied at the same time. In addition, the expression of the coupled-caloric effect is also critically dependent on the strengthening of the first-order transition nature impacted by pressure. Since the materials with the same driving directions by dual fields are very few, there is no experimental report on the coupled-caloric and multicaloric effects for such systems up to now. However, based on the obtained insights, it can be predicted that the multi-field driving cooling temperature zone will broaden in the same direction if the driving directions of the dual fields are the same. At the same time, the enhancement of the coupled-caloric effect will also innovatively contribute to the multicaloric effect. A combination of the experimental and theoretical methods mentioned above is suggested to be used to systematically study different materials. Such research not only helps to make breakthrough progress in multicaloric cycle refrigeration, but also provides valuable feedback for material developments.

References

[1] GschneidnerJr K A, Pecharsky V K and Tsokol A O 2005 *Rep. Prog. Phys.* **68** 1479
[2] Franco V, Blázquez J S, Ipus J J, Law J Y, Moreno-Ramírez L M and Conde A 2018 *Prog. Mater Sci.* **93** 112
[3] Shen B G, Sun J R, Hu F X, Zhang H W and Cheng Z H 2009 *Adv. Mater.* **21** 4545
[4] Li L W and Yan M 2020 *J. Alloys Compd.* **823** 153810
[5] Zheng X Q and Shen B G 2017 *Chin. Phys. B* **26** 027501
[6] Li Z X, Li K, Shen J, Dai W, Gao X Q, Guo X H and Gong M Q 2017 *Acta Phys. Sin.* **66** 110701 (in Chinese)
[7] Neese B, Chu B, Lu S G, Wang Y, Furman E and Zhang Q M 2008 *Science* **321** 821
[8] Manosa L and Planes A 2017 *Adv. Mater.* **29** 1603607
[9] Tušek J, Engelbrecht K, Eriksen D, Dall'Olio S, Tušek J and Pryds N 2016 *Nat. Ener.* **1** 16134
[10] Moya X, Kar-Narayan S and Mathur N D 2014 *Nat. Mater.* **13** 439
[11] Morellon L, Arnold Z, Magen C, Ritter C, Prokhnenko O, Skorokhod Y, Algarabel P A, Ibarra M R and Kamarad J 2004 *Phys. Rev. Lett.* **93** 137201
[12] Hao J Z, Hu F X, Wang J T, Shen F R, Yu Z B, Zhou H B, Wu H, Huang Q Z, Qiao K M, Wang J, He J, He L H, Sun J R and Shen B G 2020 *Chem. Mater.*
[13] Samanta T, Lepkowski D L, Saleheen A U, Shankar A, Prestigiacomo J, Dubenko I, Quetz A, Oswald I W H, McCandless G T, Chan J Y, Adams P W, Young D P, Ali N and Stadler S 2015 *Phys. Rev. B* **91** 020401
[14] Chauhan A, Patel S and Vaish R 2015 *Acta Mater.* **97** 17
[15] Liang F X, Hao J Z, Shen F R, Zhou H B, Wang J, Hu F X, He J, Sun J R and Shen B G 2019 *APL Mater.* **7** 051102
[16] Lisenkov S, Mani B K, Chang C M, Almand J and Ponomareva I 2013 *Phys. Rev. B* **87** 224101
[17] Stern-Taulats E, Castán T, Planes A, Lewis L H, Barua R, Pramanick S, Majumdar S and Mañosa L 2017 *Phys. Rev. B* **95** 104424
[18] Pecharsky V K and Gschneidner Jr. K A 1997 *Phys. Rev. Lett.* **78** 4494
[19] Hu F X, Shen B G, Sun J R and Zhang X X 2000 *Chin. Phys.* **9** 550
[20] Fujita A, Fujieda S, Hasegawa Y and Fukamichi K 2003 *Phys. Rev. B* **67** 104416
[21] Castillo-Villa P O, Soto-Parra D E, Matutes-Aquino J A, Ochoa-Gamboa R A, Planes A, Mañosa L, González-Alonso D, Stipcich M, Romero R, Ríos-Jara D and Flores-Zúñiga H 2011 *Phys. Rev. B* **83** 174109
[22] Wada H and Tanabe Y 2001 *Appl. Phys. Lett.* **79** 3302
[23] ul Hassan N, Shah I A, Khan T, Liu J, Gong Y, Miao X and Xu F 2018 *Chin. Phys. B* **27** 037504
[24] Yang H, Liu J, Li C, Wang G L, Gong Y Y and Xu F 2018 *Chin. Phys. B* **27** 107502
[25] Bao L F, Huang W D and Ren Y J 2016 *Chin. Phys. Lett.* **33** 077502
[26] Zhang H, Xing C F, Long K W, Xiao Y N, Tao K, Wang L C and Long Y 2018 *Acta Phys. Sin.* **67** 207501 (in Chinese)
[27] Zhang B, Zheng X Q, Zhao T Y, Hu F X, Sun J R and Shen B G 2018 *Chin. Phys. B* **27** 067503
[28] Trung N T, Ou Z Q, Gortenmulder T J, Tegus O, Buschow K H J and Brück E 2009 *Appl. Phys. Lett.* **94** 102513
[29] Liu J, Gottschall T, Skokov K P, Moore J D and Gutfleisch O 2012 *Nat. Mater* **11** 620

[30] Liu Y, Phillips L C, Mattana R, Bibes M, Barthelemy A and Dkhil B 2016 *Nat. Commun.* **7** 11614
[31] Liu J, Gong Y, You Y, You X, Huang B, Miao X, Xu G, Xu F and Brück E 2019 *Acta Mater.* **174** 450
[32] Qiao K, Hu F, Liu Y, Li J, Kuang H, Zhang H, Liang W, Wang J, Sun J and Shen B 2019 *Nan. Ener* **59** 285
[33] Guillou F, Pathak A K, Paudyal D, Mudryk Y, Wilhelm F, Rogalev A and Pecharsky V K 2018 *Nat. Commun.* **9** 2925
[34] Scheibel F, Gottschall T, Taubel A, Fries M, Skokov K P, Terwey A, Keune W, Ollefs K, Wende H, Farle M, Acet M, Gutfleisch O and Gruner M E 2018 *Ener. Techno* **6** 1397
[35] Liu Y, Zhang G, Li Q, Bellaiche L, Scott J F, Dkhil B and Wang Q 2016 *Phys. Rev. B* **94** 214113
[36] Planes A, Castán T and Saxena A 2014 *Philos. Mag.* **94** 1893
[37] Planes A, Castán T and Saxena A 2016 *Philos. Trans. R. Soc. A* **374** 20150304
[38] Chauhan A, Patel S and Vaish R 2015 *Acta Mater.* **89** 384
[39] Li L W 2016 *Chin. Phys. B* **25** 037502
[40] Zheng X Q, Shen J, Hu F X, Sun J R and Shen B G 2016 *Acta Phys. Sin.* **65** 217502 (in Chinese)
[41] Zhang Y 2019 *J. Alloys Compd.* **787** 1173
[42] Hao Z H, Wang H Y, Zhang Q and Mo Z J 2018 *Acta Phys. Sin.* **67** 247502 (in Chinese)
[43] Wu X F, Guo C P, Cheng G, Li C R, Wang J, Du Y S, Rao G H and Du Z M 2019 *Chin. Phys. B* **28** 057502
[44] Mo Z J, Sun Q L, Shen J, Yang M, Li Y J, Li L, Liu G D, Tang C C and Meng F B 2018 *Chin. Phys. B* **27** 017501
[45] De Sousa V, Von Ranke P and Gandra F 2011 *J. Appl. Phys.* **109** 063904
[46] Li L W, Yuan Y, Xu C, Qi Y and Zhou S Q 2017 *AIP Adv.* **7** 056401
[47] Wang X, Wang L, Ma Q, Sun G, Zhang Y and Cui J 2017 *J. Alloys Compd.* **694** 613
[48] Chen J, Zheng X Q, Dong Q Y, Sun J R and Shen B G 2011 *Appl. Phys. Lett.* **99**
[49] Delyagin N N, Krylov V I and Rozantsev I N 2007 *J. Magn. Magn. Mater.* **308** 74
[50] Chen J, Zheng X Q, Dong Q Y, Sun J R and Shen B G 2011 *Appl. Phys. Lett.* **99** 122503
[51] Zheng X Q, Chen J, Xu Z Y, Mo Z J, Hu F X, Sun J R and Shen B G 2014 *J. Appl. Phys.* **115** 17A938
[52] Ma Y F, Tang B Z, Xia L and Ding D 2016 *Chin. Phys. Lett.* **33** 126101
[53] Wu C, Ding D and Xia L 2016 *Chin. Phys. Lett.* **33** 016102
[54] Chen X and Zhao M H 2018 *Acta Phys. Sin.* **67** 197501 (in Chinese)
[55] Zhang H and Shen B G 2015 *Chin. Phys. B* **24** 127504
[56] Dong Q, Shen B, Chen J, Shen J, Zhang H and Sun J 2009 *J. Appl. Phys.* **105** 07A305
[57] Klimczak M and Talik E 2010 *J. Phys.: Conf. Ser.* **200** 092009
[58] Kaštil J, Javorský P, Kamarad J, Diop L, Isnard O and Arnold Z 2014 *Intermetallics* **54** 15
[59] Fickenscher T, Rodewald U C, Niepmann D, Mishra R, Eschen M and Pöttgen R 2005 *Z. Naturforsch. B* **60** 271
[60] Ding D, Zhang Y Q and Xia L 2015 *Chin. Phys. Lett.* **32** 106101
[61] Dong X, Feng J, Yi Y and Li L 2018 *J. Appl. Phys.* **124** 093901
[62] Fisher I, Islam Z and Canfield P 1999 *J. Magn. Magn. Mater.* **202** 1
[63] Hermes W, Rodewald U C and Pöttgen R 2010 *J. Appl. Phys.* **108** 113919
[64] Li L, Niehaus O, Kersting M and Pöttgen R 2015 *Intermetallics* **62** 17
[65] Li L, Nishimura K, Kadonaga M, Qian Z and Huo D 2011 *J. Appl. Phys.* **110** 043912
[66] Lisenkov S and Ponomareva I 2012 *Phys. Rev. B* **86** 104103
[67] Ponomareva I and Lisenkov S 2012 *Phys. Rev. Lett.* **108** 167604
[68] Planes A, Stern-Taulats E, Castán T, Vives E, Mañosa L and Saxena A 2015 *Mater. Toda.: Procee* **2** S477
[69] Meng H, Li B, Ren W and Zhang Z 2013 *Phys. Lett. A* **377** 567
[70] Nikitin S A, Myalikgulyev G, Tishin A M, Annaorazov M P, Asatryan K A and Tyurin A L 1990 *Phys. Lett. A* **148** 363
[71] Nikitin S A, Myalikgulyev G, Annaorazov M P, Tyurin A L, Myndyev R W and Akopyan S A 1992 *Phys. Lett. A* **171** 234
[72] Stern-Taulats E, Planes A, Lloveras P, Barrio M, Tamarit J L, Pramanick S, Majumdar S, Frontera C and Mañosa L 2014 *Phys. Rev. B* **89** 214105
[73] Kübler J, William A R and Sommers C B 1983 *Phys. Rev. B* **28** 1745
[74] Kainuma R, Imano Y, Ito W, Sutou Y, Morito H, Okamoto S, Kitakami O, Oikawa K, Fujita A, Kanomata T and Ishida K 2006 *Nature* **439** 957
[75] Krenke T, Duman E, Acet M, Wassermann E F, Moya X, Manosa L and Planes A 2005 *Nat. Mater.* **4** 450
[76] Yu S Y, Liu Z H, Liu G D, Chen J L, Cao Z X, Wu G H, Zhang B and Zhang X X 2006 *Appl. Phys. Lett.* **89** 162503
[77] Sharma V K, Chattopadhyay M K and Roy S B 2011 *J. Phys.: Condens Matter* **23** 366001
[78] Quetz A, Koshkid'ko Y S, Titov I, Rodionov I, Pandey S, Aryal A, Ibarra-Gaytan P J, Prudnikov V, Granovsky A, Dubenko I, Samanta T, Cwik J, Sánchez Llamazares J L, Stadler S, Lähderanta E and Ali N 2016 *J. Alloys Compd.* **683** 139